Supplemental Material to the article

"Formation of Solitary Microstructure and Ablation into Transparent Dielectric under Subnanosecond Laser Action"

Simulations are done using physical model and code described in N.A. Inogamov, V.V. Zhakhovskii, and V.A. Khokhlov, J. Exp. Theor. Phys. **127**, 79 (2018); https://doi.org/10.1134/S1063776118070075. Our subnanosecond pulse has duration 50 ps (e-folding time). For such rather long pulses the two-temperature effects are unimportant. Therefore we put $T_e = T_i$ and use our two-temperature hydrodynamic code (2T-HD) in the one temperature regime.

Formation of an overheated layer near the contact and integral dynamics. Figures S1, S2, and S3 present materials additional to Fig. 5 in the main text where the instant profiles of densities are shown for the instant $t = 150\,\text{ps}$ and the $F_{abs} = 559$ and $897\,\text{mJ/cm}^2$ cases. Figures S1, S2, and S3 demonstrate the way of gradual formation of the heated layer near the contact with the substance which strongly resists to expansion of hot Au thus gradually decelerating expansion of gold (Au). Pressure balance at the thermal front in the point 4 in Fig. S1, S2, and 5 (main text) between hot and less hot neighboring parts of Au is $\rho_h T_h \approx \rho_l T_l$ since ideal gas approximation is approximately valid. Thus temperature increase ten times causes density decrease in the same number of times.

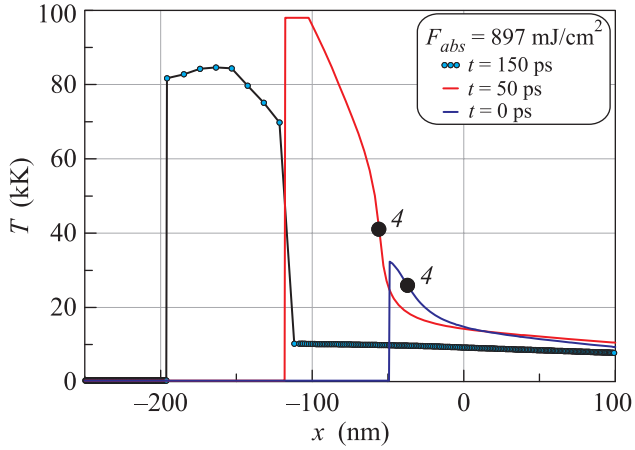

Fig. S1. The instant temperature profiles at the time range covering the laser heating process and some time after heating. We see how overheating gradually develops as heat conduction is not able to transport all of absorbed heat out of the heated layer. The overheated layer locates between the contact and the thermal front *4*. Thermal wave tries to transport absorbed energy out from the very hot contact layer of Au. The inflection point of the temperature profile is marked by the digit *4*. With time the front *4* becomes more and more steep. There is a steep increase of temperature like a jump formed to the instant $t = 150\,\text{ps}$. Thus you can put the point *4* arbitrary inside the two nodes bounding the temperature jump at the instant $t = 150\,\text{ps}$. The mesh of Lagrangian nodes is shown here at the profile $t = 150\,\text{ps}$ and in next Fig. S2 at the same profile. The heated layer is compressed by an expanding gold and a surrounding medium resisting against expansion of Au, see pressures in next two figures

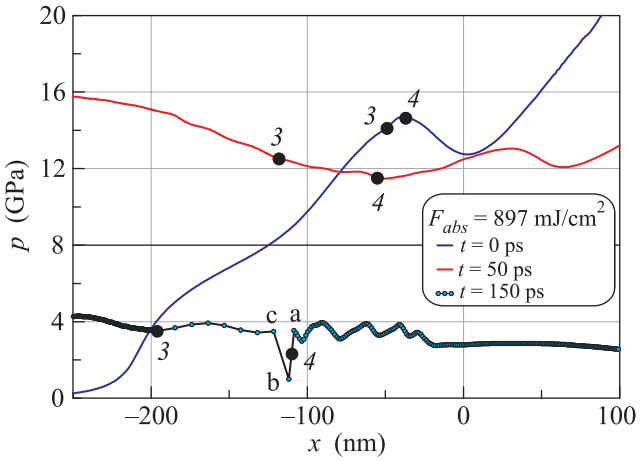

Fig. S2. Pressure profiles corresponding to the times presented in Fig. S1, also they have the same colors. We see how pressure of expanding internal gold layers compresses the heated layer *3*–*4* and further compresses the transparent matter to the left outside the contact boundary. The digits *3* and *4* mark the contact and approximate instant position of the thermal wave penetrating in direction to the internal layers of Au, respectively. We take the inflection points *4* of the temperature profiles as the instant positions of the thermal front, see Fig. S1. At the instant $t = 0$ the points *3* and *4* are close to each other (see also previous Fig. S1), because this is just beginning of development of a near contact heated layer. At the stage before the instant $t = 150$ ps a fluctuation at the thermal point *4* appears. It is marked by the letters a, b, and c. The fluctuation includes the neighboring three nodes of the Lagrangian mesh used in our finite-difference 1D hydrodynamic code. The chain of nodes is shown by the small blue circles

Figure S3 shows how energy absorbed during the subnanosecond laser pulse in the region near the point $x = 0$ creates momentum moving later the matter to the left and to the right sides relative to the absorption layer. Let's consider first the motion to the left side.

In glass we see that the compression wave develops thanks to the contact pushing a glass substance as a piston. This is shown in Fig. S3. Later in time the compression wave in glass becomes steeper and steeper. Finally this wave overtakes due to focusing of acoustic characteristics. The shock wave (SW) forms after overtaking; this phenomenon is called also wave breaking.

As follows from Fig. S3, formation of the shock takes place between the instants $t = 0$ (half of a heating laser pulse is absorbed) and $t = 50\,\text{ps}$ – the heating is practically finished – e-folding time of our pulse is $\tau_L = 50\,\text{ps}$: $I(t) = I_0 \exp(-t^2/\tau_L^2)$. 92 % of totally absorbed energy is absorbed to the instant $t = 50\,\text{ps}$. Let's pay attention to the profile corresponding to $t = 50\,\text{ps}$ – the red curve in Fig. S3. We see a powerful hill of compression just behind the newly formed shock. This hill moves faster relative to glass substance behind the shock than the shock itself because motion behind a shock is subsonic. This hill appears thanks to rather long laser action with $\tau_L = 50\,\text{ps}$. Long action pumps and pumps pressure near absorbing contact while the first characteristics run ahead the contact, intersect, and form a shock. We don't see such a hill in simulations with ultrashort durations. The hill is gradually absorbed by the

shock amplifying the shock at the time interval between the instants 50 and 150 ps: compare the amplitudes of the pressure jump at the shock front at these instants.

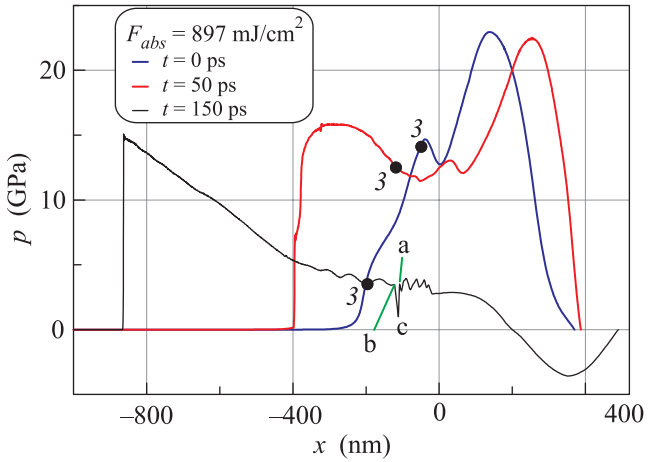

Fig. S3. The whole picture of expansion of the Au film to the left and right. Colors of the pressure profiles are the same as in Fig. S1 and S2. From the left side the Au film is bound by a glass semi-space. At the right side the film is separated from vacuum by the vacuum boundary. The points *3* show instant position of the contact during expansion process of Au. The points a, b, and c bound the fluctuation appearing to the instant 150 ps at the thermal front *4* shown in previous Fig. S1 and S2. The whole in space and time picture consists from the formation and propagation of a shock in glass and expansion of a film initially 370 nm thick. The pressurized layer at the left side of a film moves the rest of the film to the right. During this motion Au expands and stretches, thus in the condensed part of the film the field of tensile stresses $p < 0$ forms

During the stage between $t = 50$ and 150 ps the shock transforms from its unusual shape with a bump ($t = 50$ ps) into standard triangular shock slowly decaying $\propto t^{-1/2}$, $t \gg d_f/c_s$ as it propagates out from the contact which initially creates the compression wave. In the case of ultrashort laser action the triangular shock appears at the early stages omitting the stage with a pressure bump behind a shock (the red curve in Fig. S3).

Decay of a film into a set of spallation layers separated by a two-phase mixture. Figure S4 presents additional materials to the problem discussed in the main text around Fig. 8. These figures relates to the experiments done in [7, 8]. In the experiments the tightly focused laser beam acts onto molten gold film initially 370 nm thick.

The rather late stage $t = 0.5$ ns is shown in Fig. S4. As was said above, the absorption during the subnanosecond pulse action increases pressure around the absorbing contact. The smooth gradual in time pressure increase pushes matter to the left and to the right sides relative to the contact. The repulsion appears because total momentum of a system of dielectrics and metal was zero before the pulse, and the pulse doesn't add additional momentum to the system because we neglect momentum of photons – velocity of light c is too high relative to hydrodynamic velocities v, thus at equal energies the momentum of mass is much larger (c/v times larger) than momentum of light. The motion to the left side is described in Fig. S3. Figures S1 and S2 present formation and development of an overheated layer in gold near the contact. Figure S4 together with Fig. 8

from the main text demonstrates important features of the motion to the right side.

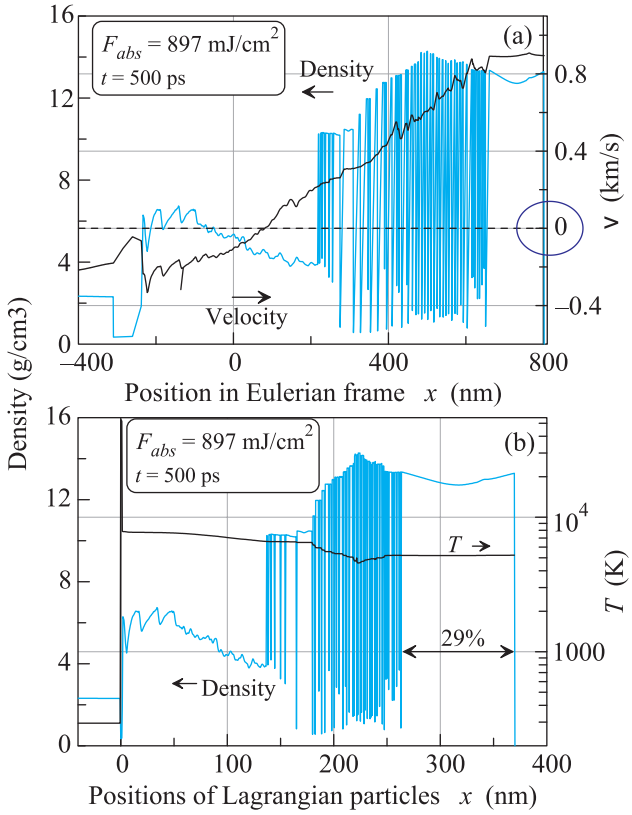

Fig. S4. (a) – Profiles of density and velocity along an Eulerian coordinate x for the instant 0.5 ns. Here we use Eulerian coordinate x as in all figures above showing the instant profiles. We see formation of the high speed external condensed matter layer moving to the vacuum side. Subsequent flight of this matter forms a fast jet seen in experiments presented in [7, 8] cited in the main text. The two-phase (vapor-liquid gold) mixture behind the external layer also contributes to the lower and slower moving parts of the jet. Thus the jet is inhomogeneous along its length. (b) – The inner parts of the Au film are hot. Their internal energies overcome sublimate energy of gold. Thus later in time they evaporate leaving the through hole up to the glass surface. The density and temperature profiles are shown along the Lagrangian coordinate x_0 marking positions of the chain of the material points along the 1D axis x before the action of laser pulse. The Lagrangian position of the particular particle does not change in time. E.g., the contact and boundary with vacuum are placed always in the same points. Distance between them is always 370 nm. With use of the Lagrangian frame we see how much matter belongs to one or another interval of motion. There is 29 % of total mass of a gold film is accumulated inside the external layer flying to vacuum at the instant 0.5 ns shown in figure. While amount of matter inside the near contact overheated layer of gold is small

The momentum directed to the right is carried through a film by the acoustic wave. When this acoustic waves reflects from the boundary with vacuum at the right edge of a film then negative pressures appear. They cause rear-side spallation. This is well known picture. But in our case an acoustic impedance

$Z = \rho c_s$ of dielectrics is low. Thus the left momentum is only partially consisted from momentum of the moving substance of dielectrics. Another part is attached to the gold near a contact. This part moves to the left thus stretching the left side of a film. This stretching induces ruptures in the left side of a film.

The ruptures at the left side proceed before the rear-side rupture because the left side is close to the heated layer – the source of the pressure increase. Therefore the series of ruptures starts from the left side. But this concerns the cases with relatively low absorbed energies 338 and 559 mJ/cm^2. The situation with multiple ruptures is shown in Fig. 8 of the main text. This figure corresponds to the case with $F_{abs} = 338\,\mathrm{mJ/cm^2}$. The situation with $F_{abs} = 559\,\mathrm{mJ/cm^2}$ is similar.

Said above relates to the cases where cohesive properties are important and the sequence of the condensed matter layers alternates (intermits) with the layers filled by a two-phase mixture. Instant velocity profile has the intervals of linear growth in the mixture $|\partial v/\partial x| > 0$ and is approximately constant (the plateaus in the velocity profile) in the condensed layers $\partial v/\partial x \approx 0$. Matter expands in the mixture (decreases density) while keeping approximately constant densities in the plateaus. In the case with the highest value of $F_{abs} = 897\,\mathrm{mJ/cm^2}$ more than a half of a film at the left side is heated so strongly that cohesive properties of gold in this side almost disappear, see Fig. S4b. We see that in the case of such strong heating the intermediate condensed layers disappear, see Fig. S4a. While the matter near the contact is heated up to the critical point values. Only the layer (or plateau) near the right edge survives.

Velocity of the right layer in Fig. S4 is high: 0.9 km/s. This layer forms a jet seen in the experiments [7, 8]. How the range of velocities from the maximum value 0.9 km/s to much lower values is formed? This is explained in the papers [9, 10] cited in the main text. If we have illumination homogeneously distributed along infinitely large contact surface then the part in the ejecta will flies with velocity 0.9 km/s. But in the experiments [7, 8] the illuminated spot has micron scale. In this case outside the maximum illumination in the central region the illumination is weaker and velocities are smaller. But all they (all which belong to the illuminated spot) are focused by capillary forces into a thin long jet, see [9, 10].

Molecular dynamics techniques. Molecular dynamics simulation of atom diffusion in the hot binary mixture Au-Water was performed with using three different potentials describing interactions between atoms Au-Au, Water-Water, and Au-Water. The new revision of embedded atom model (EAM) interatomic potential for Au-Au atoms was developed using the EAM potential presented in: V. V. Zhakhovskii, N. A. Inogamov, Yu. V. Petrov, S. I. Ashitkov, and K. Nishihara, Appl. Surf. Sci. **255**, 9592 (2009). This revised potential provides the correct surface tension and dimer energy of gold.

Water is considered in our simulation as a monatomic system, for which the EAM potential was developed in [6] of the main article, see the data files on the project url: https://www.researchgate.net/project/Development-of-interatomic- EAM-potentials. It provides the correct mechanical properties of liquid water including the density and sound speed in ambient conditions, and shock Hugoniot as well.

Due to lack of information, the interaction of Au atom and water molecule is greatly simplified to a pairwise potential between Au and "water" atoms using the van der Waals radii 0.166 nm for Au and 0.152 nm for oxygen atom, and a strong repulsion $\sim r^{-11}$ is assumed. The usage of larger van der Waals radius 0.19 nm of water for our "water" atom reduces the diffusion coefficient of Au

atoms in the simulated 50/50 binary mixture by about 10–20 %; 50/50 is on the number of atoms per unit of volume; partial densities are 4.1 and 0.4 g/cm^3 for Au and water, respectively. Results of MD simulations relating to calculations of diffusion coefficient in the overcritical states of gold are presented in Fig. 7 of the main text.